Dependence of human squat jump performance on the series elastic compliance of the triceps surae: a stimulation study

Bobbert, M.F.

DEPENDENCE OF HUMAN SQUAT JUMP PERFORMANCE ON THE SERIES ELASTIC COMPLIANCE OF THE TRICEPS SURAE: A SIMULATION STUDY

MAARTEN F. BOBBERT*

Institute for Fundamental and Clinical Human Movement Sciences, Vrije Universiteit, Van der Boechorststraat 9, 1081 BT Amsterdam, The Netherlands

*e-mail: m_f_bobbert@fbw.vu.nl

Summary

The purposes of this study were to determine the dependence of human squat jump performance on the compliance of series elastic elements (SEEs) of the triceps surae (consisting of the soleus and gastrocnemius) and to explain this dependence. Vertical squat jumps were simulated using an optimal control model of the human musculo-skeletal system. Maximum jump height was found for several values of triceps surae SEE strain at maximum isometric force (ε_0). When ε_0 was increased from 1 to 10 %, maximum jump height increased by 8 cm. This was partly due to a higher work output of contractile elements (CEs) of the muscles, primarily of the soleus, and also partly to an increased efficacy of converting muscle work to energy contributing to jump height. The soleus produced more work at ε_0=10 % because, as a result of SEE recoil, the CE covered its shortening range at lower velocity and hence produced more force. Efficacy was higher at ε_0=10 % because a higher vertical velocity at take-off was achieved with a lower rotational energy of the body segments. This apparent discrepancy was explained by increased angular velocities of the shanks and feet, which have small moments of inertia, and decreased angular velocities of the thighs and trunk, which have larger moments of inertia. This redistribution of segmental contributions to the vertical velocity of the centre of mass was possible because the increased compliance of the triceps surae SEE enhanced the energy-buffering capacity of this muscle group and, thereby, allowed for a higher power output at the ankles. It seems that long compliant tendons in the plantar flexors are an elegant solution to the problem of maximizing jumping performance.

Key words: musculoskeletal model, optimal control, muscle functioning, jump performance, contractile element, series elastic element, strain, human.

Introduction

The musculoskeletal system is an extremely complex structure with many levels of organization, varying from the arrangement of molecules in myofilaments to that of muscle–tendon complexes in the skeleton. It is generally acknowledged that the global design of the system is the outcome of an evolutionary process and that differences in design among species are related to differences in functional demands. Our challenge is to find relationships between design aspects and functional demands. The obvious problem with this challenge is that we do not really know for which demands a given design aspect is the solution.

One of the intriguing design aspects of the human musculoskeletal system is that distal muscle–tendon complexes, notably those of the plantar flexors, span the large distance between origin and insertion with long tendinous structures and very short muscle fibres (5–6 cm). For example, each muscle fibre of the gastrocnemius is linked to tendinous tissue with a total length of more than 35 cm. Obviously, the arrangement of many short muscle fibres in parallel allows for a large physiological cross-sectional area, and thus a large muscle force,

at the expense of the range of shortening and the maximal shortening velocity of the muscle fibres. But what is the role of the tendinous tissue? The consensus of opinion is that tendinous tissue does not simply transfer muscle forces to the skeleton. It is compliant and can therefore also store and release energy. It has been argued that this mechanism may help to increase efficiency during so-called stretch–shortening exercises such as running, in which active muscles are stretched prior to shortening (e.g. Cavagna, 1977; Minetti et al., 1999). It has also been argued that storage of elastic energy during a pre-stretch may help to increase the maximum work produced during shortening over that produced without pre-stretch (Asmussen and Bonde-Petersen, 1974; Komi and Bosco, 1978; Svantesson et al., 1991). This latter argument, however, has been refuted (Bobbert et al., 1996; van Ingen Schenau et al., 1997) because, when the length of a muscle–tendon complex (MTC) at the start of shortening is fixed, storage of elastic energy requires lengthening of series elastic elements (SEEs), and such lengthening can occur only at the expense of the potential shortening distance of contractile elements.

The compliance of series elastic structures may not affect maximum work output during shortening of an MTC, but it will affect the rate at which energy can be released. Using a model of the triceps surae MTC driven by muscle stimulation and kinematic patterns measured during human jumping, it has been shown that a large compliance of the SEE of the triceps surae MTC is required to explain the high power output measured at the ankle (Bobbert et al., 1986b). Achieving a high power output about the ankle, in turn, was argued to be of crucial importance in jumping (Bobbert et al., 1986b). These arguments were tested in optimal control studies using a forward dynamic model of the musculoskeletal system (Anderson and Pandy, 1993; Pandy, 1990; Pandy et al., 1990). In that model, the tendinous tissue was characterized by a linear stress/strain relationship with values for the strain of the SEE at maximum isometric force (ε_0) of 2.5–5.3 % (Pandy et al., 1990). Anderson and Pandy (Anderson and Pandy, 1993) found that increasing ε_0 of the proximal MTCs (vasti, rectus femoris, glutei and hamstrings) to the physiological limit of 10 % produced only a 3 % increase in maximum jump height (which was 65 cm in that study). This led them to conclude that SEE compliance did not affect jump height significantly. Pandy (1990) also found that increasing ε_0 of the plantar flexors (soleus and gastrocnemius) from 2.6 to 10 % caused squat jump height to increase from 33 to 40.5 cm (Pandy, 1990). Despite this 23 % increase in performance, Pandy (1990) again concluded that the contribution of SEE compliance to jumping performance was negligible, probably because the effect of a particular relative change in SEE compliance (i.e. a change expressed as a fraction of the reference value) was small compared with the effect of the same relative change in other variables (such as the maximal shortening velocity of muscle fibres and the body strength to weight ratio), and probably also because Pandy (Pandy, 1990) felt that a value of 10 % for ε_0 was far from realistic.

So, from the above studies, the general consensus is that jump height is insensitive to changes in SEE compliance (Zajac, 1993). However, we feel that that this may not be correct for several reasons. First, the effect of a change in compliance from the reference value does not provide information on the role of that compliance at the reference value. Second, recent studies suggest that high values for SEE compliance are in fact realistic. In one of these studies (Hof, 1998), subjects first produced a voluntary isometric contraction with their triceps surae in a dynamometer. When the force had reached a plateau, the dynamometer rapidly rotated the foot, imposing a shortening velocity on the triceps surae MTC much higher than the maximum shortening velocity of the contractile elements. The shortening distance at which the force was reduced to zero was determined. Hof (Hof, 1998) concluded that, at maximum isometric force, series elastic structures could be stretched by 3.6 cm, implying a strain of approximately 10 %. Similarly high values for SEE compliance may be derived for the vastus lateralis from ultrasonography data (Kubo et al., 1999).

The purposes of the present study were to investigate further the dependence of squat jump performance on the compliance of the tendinous tissue of the triceps surae and to try to explain this dependence. To this end, an optimal control approach was used with a model of the musculoskeletal system. Simulation results were compared with data collected during maximum-height squat jumps of a human subject.

Materials and methods
Experimental data

To acquire initial conditions for simulations and to evaluate simulation results, we used kinematic and kinetic data from an experienced male jumper (mass 85 kg, height 1.91 m) performing maximum-height squat jumps. These data were collected as part of a study described in detail elsewhere (Bobbert et al., 1996). Briefly, the subject started his jumps from a semi-squatting position and was instructed to make no countermovements. Sagittal plane coordinates of markers placed at the height of the neck, hip joint, knee joint, ankle joint and fifth metatarsophalangeal joint were obtained using a VICON high-speed video-analysis system (Oxford Metrics Ltd, Oxford, UK) operating at 200 frames s^{-1}. Ground reaction forces produced during jumping were measured using a Kistler force platform (type 9281B, Kistler Instrument Corp., Amherst, NY, USA) and sampled simultaneously with the kinematic data. From the positional data, we calculated jump height, defined as the difference between the height of the centre of mass of the body at the apex of the jump and the height of this centre of mass when the subject was standing upright with the heels on the ground. The highest of three squat jumps was selected for further analysis. Net joint moments, power output and work were obtained by performing an inverse-dynamics analysis (Elftman, 1939), combining kinematic information and ground reaction forces.

Simulation model

For the simulations, we used the two-dimensional forward dynamic model of the human musculoskeletal system shown in Fig. 1. The model, which calculated internal states and MTC forces as well as the motion of body segments corresponding to stimulation-time input of the muscles, has been described in detail elsewhere (van Soest et al., 1993). It consisted of three rigid segments, representing the feet (F), shanks (S) and thighs (T), and a fourth rigid segment representing the head, arms and trunk (HAT). The segments were interconnected by hinge joints representing the hip, knee and ankle joints. In the skeletal submodel, which had a total mass of 82 kg, the following six major MTCs contributing to extension of the lower extremity were embedded: hamstrings, gluteus maximus, rectus femoris, vasti, gastrocnemius and soleus. The six MTCs were represented using a Hill-type muscle model (Hill, 1938). This model consisted of a contractile element (CE), a series elastic element (SEE) and a parallel elastic element (PEE) and has also been described in detail elsewhere (van Soest and Bobbert, 1993). Briefly, the behaviour of the SEE and PEE was determined by a quadratic force–length relationship. The
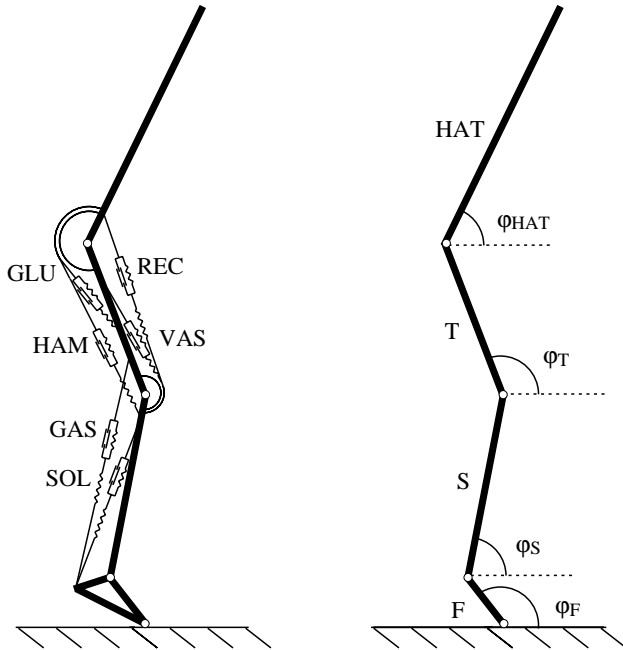
Fig. 1. Schematic drawing of the model of the musculoskeletal system used in forward dynamic simulations. The model consists of four interconnected rigid segments (feet, F; shanks, S; thighs, T; and a HAT segment representing the head, arms and trunk) and six muscle–tendon complexes of the lower extremity (hamstrings HAM, gluteus maximus GLU, rectus femoris REC, vasti VAS, gastrocnemius GAS and soleus SOL), all represented by Hill-type muscle models. Segment angles φ_{HAT}, φ_T, φ_S and φ_F are all expressed relative to the right-hand horizontal.

where V is shortening velocity, F_0 is maximum isometric force, and a and b are constants. In the present study, V was replaced by $-\dot{l}_{CE}$, and F_0 was replaced by $F_{max}f_{isom}q$, where F_{max} is the maximum isometric force of the muscle at maximum active state ($q=1$) and optimum CE length ($l_{CE,opt}$), and f_{isom} indicates which fraction of this force can be produced at other CE lengths (see below). For further details of this formulation, and of the formulation of the eccentric part of the force–velocity relationship, which played a negligible role in the present study, the reader is referred to van Soest and Bobbert (van Soest and Bobbert, 1993).

The parameters of the model were not tuned to represent individual subjects, but only to represent a group of subjects (Bobbert et al., 1996; van Soest and Bobbert, 1993; van Soest et al., 1993). The values of variables derived for the soleus and gastrocnemius MTCs are presented in Table 1. For the present study, it is relevant to mention a few of the conceptual steps made in deriving these values. First, an MTC was regarded as a collection of identical units, each composed of a muscle fibre made up of identical sarcomeres in series, and a 'tendon fibre' bridging the gap between the muscle fibre and the centroids of origin and insertion (Bobbert et al., 1986a; Bobbert et al., 1990). Second, it was assumed that the muscle fibres were responsible for the properties of the CE and PEE, and the 'tendon fibres' for those of the SEE. Thus, the series elasticity residing in the muscle fibres themselves was neglected relative to that of the tendinous tissue (for the MTC as a whole this seems reasonable, because the length of the muscle fibres is small compared with that of the tendinous tissue in series with them). Given the properties of each sarcomere and the stiffness properties of tendinous tissue, making the assumptions mentioned above allowed us to derive values for the variables describing the behaviour of the MTC from (i) the number of sarcomeres in series in each muscle fibre, (ii) the origin-to-insertion distance at which the MTC attains its optimal length (i.e. the length at which it produces its maximum isometric force) and, in theory but not in practice (see below), (iii) the number of sarcomeres in parallel in the whole MTC.

The relationship between f_{isom} and the length of a sarcomere was modelled as an inverted parabola with zero values below 0.44 and above 1.56 times sarcomere optimum length (Bobbert et al., 1986a). The force of a 'tendon fibre' was assumed to be zero below slack length and to increase quadratically to

behaviour of the CE was more complex: CE contraction velocity $\dot{l}_{CE}$ depended on active state q, CE length l_{CE} and force F. Following Hatze (Hatze, 1981), the relationship between q (essentially representing the relative amount of Ca^{2+} bound to troponin) and muscle stimulation STIM was modelled as a first-order process. STIM, ranging between 0 and 1, is a one-dimensional representation of the effects of the recruitment and firing frequency of α-motoneurons. The description of the relationship between contraction velocity and force was based on Hill's equation (Hill, 1938):

$$(F + a)(V + b) = (F_0 + a)b, \qquad (1)$$

Table 1. *Values for selected variables for the soleus (SOL) and gastrocnemius (GAS) muscles used in the model*

	$l_{CE,opt}$ (m)	$V_{CE,max}$ (m s^{-1})	$l_{SE,0}$ (m)	F_{max} (N)	$P_{CE,max}$ (W)	d_{ankle} (m)	d_{knee} (m)
SOL	0.055	0.70	0.235	8000	685	0.046	0
GAS	0.061	0.77	0.364	4000	380	0.046	0.017

Force and power values are for two legs together.

$l_{CE,opt}$, optimum length of muscle fibres (contractile elements, CE); $V_{CE,max}$, maximal shortening velocity of contractile elements at maximum active state and $l_{CE,opt}$; $l_{SE,0}$, greatest length of series elastic element at which force is still zero; F_{max}, maximum isometric force (at $l_{CE,opt}$); $P_{CE,max}$, maximum power output of contractile elements at maximum active state and $l_{CE,opt}$; d_{ankle}, average moment arm at ankle during simulations; d_{knee}, average moment arm at knee during simulations.

isometric muscle force at a strain ε_0, which was 4% in the reference model. To describe the relationship between the force and concentric velocity of a sarcomere, a/F_{max} and $b/l_{CE,opt}$ were set to 0.41 and $5.2\,s^{-1}$, respectively (Bobbert et al., 1986b). The numbers of sarcomeres observed in series for the soleus and gastrocnemius in human cadavers, 16 270 and 17 825, respectively (P. A. Huijing, personal communication), were adjusted for shank length.

Values for absolute muscle forces and tendon fibre slack lengths were estimated as follows. The physiological cross-sectional areas of muscles (a measure of the number of sarcomeres in parallel), defined as muscle volume divided by muscle fibre optimal length, were determined in human cadavers (P. A. Huijing, personal communication). The ratio of maximal isometric forces of the muscles crossing a joint was set equal to the ratio of physiological cross-sectional areas. The ratio SOL:GAS was determined to be 2:1. Using an optimization procedure, the tendon fibre slack lengths of the muscles crossing a joint were subsequently adjusted in such a way that the best fit was obtained between the maximum isometric moment-angle relationship of the model and relationships measured in maximum isometric contractions of subjects on a dynamometer (Out et al., 1996).

At the start of each simulation, the model was put in the starting position selected by the subject, and the initial STIM levels of the mono-articular glutei, vasti and soleus were set such that static equilibrium was achieved. Subsequently, STIM was allowed to switch only once from this initial value to the maximal value of 1.0 and thereafter had to remain maximal until take-off. Under this restriction, the motion of the body segments, and therewith the performance of the model, depended on six variables: the instants at which the STIM of each of the six MTCs switched from the initial value to the maximal value. Thus, an optimization problem could be formulated: what combination of six switching times produced the maximum value of the height achieved by the centre of mass (CM)? This problem was solved with the help of a genetic algorithm (L. J. R. Casius and A. J. van Soest, in preparation). For each condition, the optimization ran for 500 generations of a population of 100 chromosomes, each of which was a bit-string coding one combination of the six stimulation onset times.

The dynamic optimization problem was solved for different values of ε_0: 1%, 4%, 10%, 15% and 20%, with 4% being the reference value used in our previous simulation studies. When ε_0 was adjusted, the slack length of the SEE was not adjusted. Thus, in the static equilibrium position, the amount of elastic energy stored in the SEE of the soleus increased with ε_0, but the extra energy was essentially produced by the CE. In trying to explain the effects of changing SEE compliance on jump height, we shall focus on the differences between $\varepsilon_0=4\%$ and $\varepsilon_0=10\%$.

Results and discussion

Comparison of experimental and simulation results

Fig. 2A shows experimental data for the maximum-height squat jump of the subject. Fig. 2B shows the results from the

Fig. 2. Stick diagrams for the push-off in maximum-height squat jumping for a subject (A) and for the optimal solutions of the simulation model with the strain at maximum isometric force ε_0 of the series elastic elements of the triceps surae set to 4% (B) or 10% (C). In each panel, the leftmost stick diagram depicts the position at the start of upward motion of the centre of mass, the rightmost one the configuration at the last frame before take-off, and the intermediate diagrams are spaced 50 ms apart, counting backwards from the instant of take-off ($t=0\,s$). In each stick diagram, the ground reaction force vector (lower arrow) is represented with its origin at the centre of pressure, and the velocity vector of the centre of mass (upper arrow) is shown with its origin at the location of the centre of mass. The broken vertical line represents the stationary environment and is added for easy reference.

maximum-height squat jump of the reference model (ε_0=4 %) obtained by optimization of stimulation onset times. In Fig. 2C, results are shown for the maximum-height squat jump of the model with increased SEE compliance of the triceps surae (ε_0=10 %). Fig. 3 presents, for both the subject and the model, time histories of segment angles (see definitions in Fig. 1), and Fig. 4 presents time histories for power production at the joints.

Overall, a good correspondence was obtained between the kinematics of the jumps of the model and those of the subject (Figs 2, 3), as in other simulation studies (Anderson and Pandy, 1993; Pandy et al., 1990; van Soest et al., 1993). The subject's jump height was, however, greater than the maximal jump height of the model. This is a general finding, which is primarily explained by the fact that, in contrast to the model, subjects do not have a rigid trunk and can use the muscles of the back to contribute work (van Soest et al., 1993). The kinematics of the subject was modelled more accurately by the simulated jump with ε_0=10 % than with ε_0=4 % (Figs 2, 3). For example, rotations of the feet and shanks occurred later in the subject and in the model with ε_0=10 % than in the model with ε_0=4 %. Moreover, peak power output at the ankle joints (Fig. 4) and the jump height of the subject (Fig. 2) were more similar using the model with ε_0=10 % than with ε_0=4 %. Note that, with ε_0=10 %, peak power output at the ankle was 1800 W, almost twice the theoretical maximum power output of the muscle fibres of the triceps surae (Table 1). Note also that, in the simulated jumps, power production at the knee and hip joint did not drop to negative values shortly before take-off, as was the case for the subject. This may well be because no anatomical constraints were included in the model, while the subject, of course, will try to prevent damage to the passive structures that limit the joint range of motion (van Ingen Schenau et al., 1987). The subject can do this by deactivating hip and knee extensor muscles and activating mono-articular hip and knee flexor muscles to dissipate rotational energy just before take-off. Including anatomical constraints in the model would involve adding such muscles and changing the optimization criterion. This was not attempted; considering the overall correspondence between the experimental and simulation results (Figs 2–4), it was felt that the present model sufficiently captured the salient features of the real system and adequately simulated vertical jumping.

The effects of changing the SEE compliance of the triceps surae on performance

Table 2 presents information on a few selected variables related to energy, work and their constituents for a number of simulated jumps with different values for ε_0. It is clear that ε_0 has a considerable effect on squat jumping performance: variations in maximum jump height of approximately 9 cm were achieved by changing triceps surae SEE compliance. Surprisingly, the changes in jump height were not only due to changes in the work output of the MTCs. For example, the increase of 4 cm realized when ε_0 was increased from 4 to 10 % corresponds to an extra amount of effective energy of 29.7 J, whereas the extra amount of work produced during the push-off was only 20.8 J.
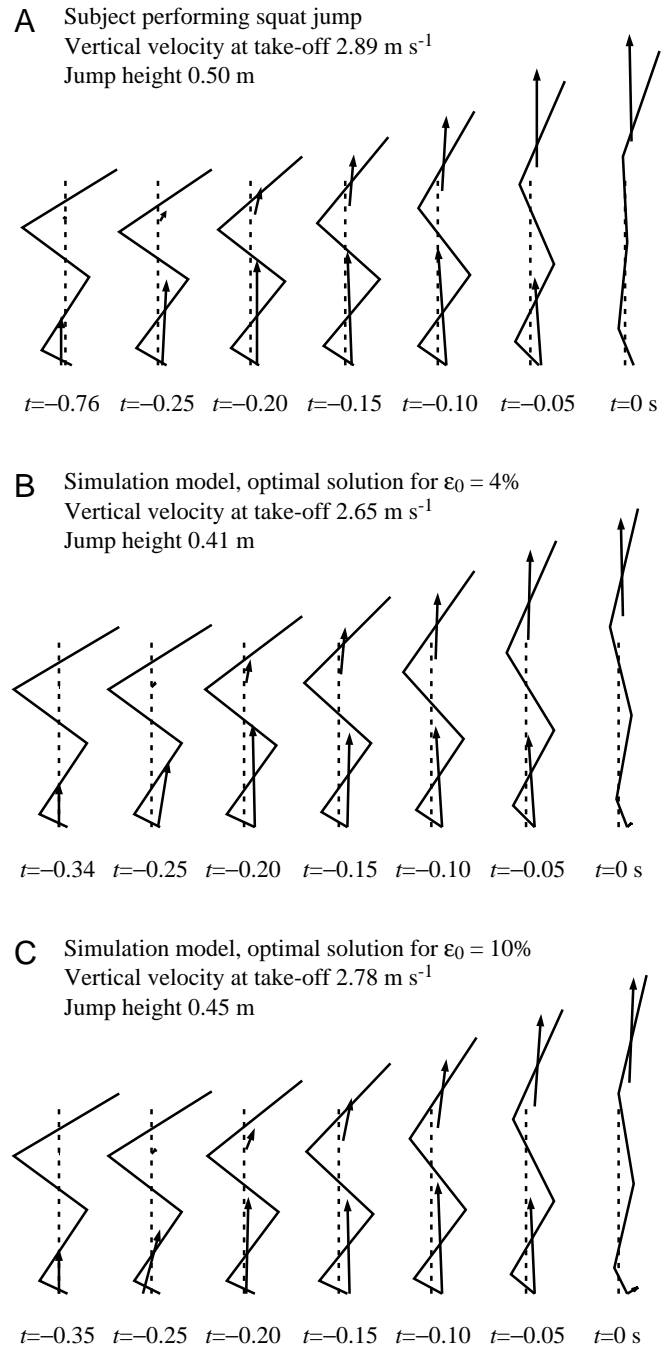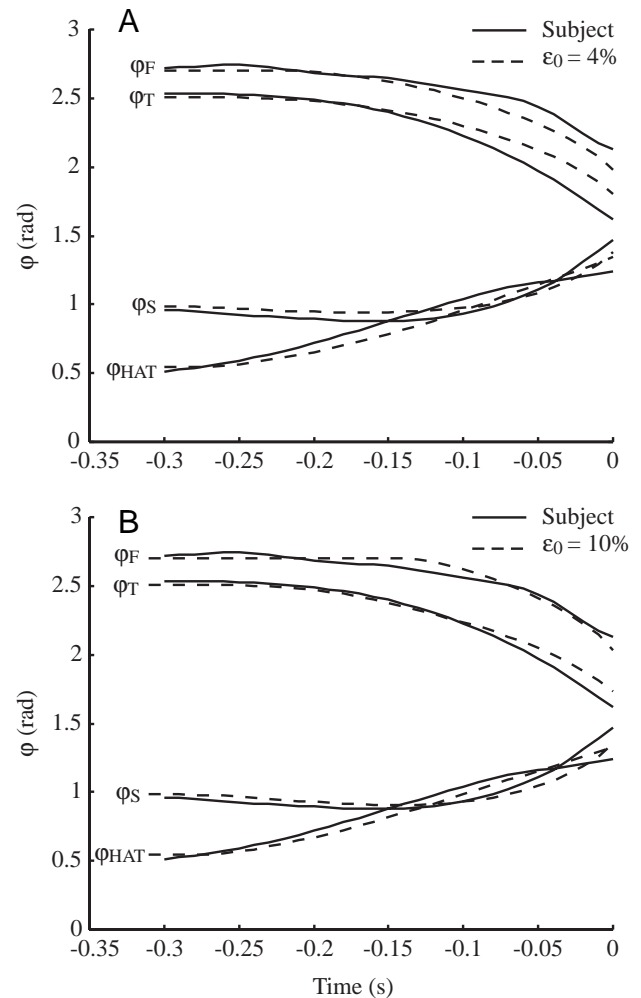

Fig. 3. Time histories of segment angles (φ) for the push-off in maximum-height squat jumping for a subject (solid lines) and for the optimal solution of the simulation model with the strain at maximum isometric force ε_0 of the series elastic elements of the triceps surae (broken lines) set to 4 % (A) or 10 % (B). φ_F, φ_S, φ_T and φ_{HAT} represent, respectively, the angles relative to the right horizontal of the feet F, shanks S, thighs T and the head, arms and trunk segment (HAT) (see definitions in Fig. 1). Take-off is at t=0 s.

Apparently, there was also an increase in the efficacy ratio, defined as the ratio of effective energy output (energy contributing to jump height) to work done. Below, I shall attempt first to identify the source of the extra work produced and subsequently to explain why the efficacy was increased.

Why does a change in the SEE compliance of the triceps surae affect the amount of work produced?

Table 3 presents information on stimulation onset times of the MTCs, work produced by the MTCs and work contributions of the CE and SEE for simulated jumps with ε_0=4 % and ε_0=10 %. The increase in the amount of work produced at ε_0=10 % was due primarily to an increase in the work output of the soleus, whose SEE compliance was changed, but also to changes in the work output of other MTCs.

Table 2. *Values for selected variables related to energy, work and their constituents for a number of simulated jumps with different values for the strain at maximum isometric force ε_0 of the series elastic elements of the triceps surae*

	$\Delta z_{CM,start}$ (m)	$\Delta z_{CM,to}$ (m)	$\Delta z_{CM,max}$ (m)	$\Delta E_{pot,to}$ (J)	$\dot{z}_{CM,to}$ (m s^{-1})	$E^z_{kin,to}$ (J)	$\sum_{i=1}^4 E^z_{rot,to,i}$ (J)	$\Delta E_{eff,to}$ (J)	W_{tot} (J)
$\varepsilon_0=1\%$	0	0	−0.04	+0.5	−0.14	−29.0	+6.9	−28.5	−20.3
$\varepsilon_0=4\%$	**−0.33**	**0.05**	**0.41**	**307.3**	**2.65**	**288.1**	**66.1**	**595.4**	**685.7**
$\varepsilon_0=10\%$	0	0	+0.04	−0.2	+0.13	+29.9	−8.1	+29.7	+20.8
$\varepsilon_0=15\%$	0	0	+0.05	+0.7	+0.19	+42.8	−3.8	+43.5	+33.3
$\varepsilon_0=20\%$	0	+0.01	+0.02	+4.2	+0.05	+11.7	−8.6	+15.9	−1.5

Absolute values are presented for $\varepsilon_0=4\%$ (in bold type), and values obtained with other values ε_0 are expressed relative to those at $\varepsilon_0=4\%$.

$\Delta z_{CM,start}$, initial height of centre of mass (CM) relative to height of CM in upright standing; $\Delta z_{CM,to}$, height of CM at take-off relative to height of CM in upright standing; $\Delta z_{CM,max}$, jump height, i.e. maximum height of CM relative to height of CM in upright standing, $\Delta E_{pot,to}$, potential energy at take-off relative to potential energy in starting position; $\dot{z}_{CM,to}$, vertical velocity of CM at take-off; $E^z_{kin,to}$, kinetic energy due to vertical velocity of CM at take-off; $\sum_{i=1}^4 E^z_{rot,to,i}$, sum of rotational energies of segments at take-off; $\Delta E_{eff,to}$, increase in effective energy during push-off (sum of $\Delta E_{pot,to}$ and $E^z_{kin,to}$); W_{tot}, total work output of muscle–tendon complexes during push-off.

Table 3. *Values for optimal stimulation onset times of the muscle–tendon complexes of the model, work produced by the muscle–tendon complexes and the contributions to this work by contractile element and series elastic element*

		SOL	GAS	VAS	REC	GLU	HAM	Total
$\varepsilon_0=4\%$	t_{onset} (s)	**0.036**	**0.017**	**0.047**	**0.162**	**0.010**	**0**	
	W_{CE} (J)	**83.4**	**50.5**	**168.6**	**15.2**	**241.6**	**124.4**	**683.7**
	W_{SEE} (J)	**3.7**	**−0.7**	**2.8**	**−5.0**	**2.0**	**−0.8**	**2.0**
	W_{tot} (J)	**87.1**	**49.8**	**171.4**	**10.2**	**243.6**	**123.6**	**685.7**
$\varepsilon_0=10\%$	t_{onset} (s)	+0.023	+0.105	+0.004	−0.013	+0.010	0	
	W_{CE} (J)	+6.4	+2.2	+2.0	+1.0	+5.4	−0.4	+16.6
	W_{SEE} (J)	+6.1	−3.0	+0.1	+0.6	+0.1	+0.4	+4.2
	W_{tot} (J)	+12.5	−0.8	+2.1	+1.5	+5.5	0	+20.8

Absolute values are presented for the model with the strain at maximum isometric force ε_0 of the series elastic elements of the triceps surae set to 4%.

Values obtained at $\varepsilon_0=10\%$ are expressed relative to those obtained at $\varepsilon_0=4\%$ (in bold type).

Work values are for two legs together.

SOL, soleus; GAS, gastrocnemius; VAS, vasti; REC, rectus femoris; GLU, gluteus maximus; HAM, hamstrings; t_{onset}, instant at which stimulation switched from the initial value to the maximum value; W_{CE}, W_{SEE}, W_{tot}, net work output of contractile element, series elastic element and total muscle–tendon complex, respectively.

The increase in work output of the soleus MTC when ε_0 of the triceps surae SEE was increased from 4 to 10% was due to a reduction in soleus CE shortening velocity V_{CE}, which in turn was due to a higher contribution of the SEE to the MTC shortening velocity. Fig. 5A shows the force produced by the soleus as a function of soleus MTC length for these two conditions. In both cases, a slight stretch of the MTC occurred initially. This was due to a slight clockwise rotation of the shanks (Figs 2, 3) caused by the later stimulation onsets of the plantar flexors and the vasti than of the glutei and hamstrings (Table 3). With $\varepsilon_0=10\%$, the amplitude of the stretch was a little larger because the plantar flexors were activated later (Table 3). Fig. 5B shows the force produced by the soleus as a function of soleus CE length. It can be seen that the initial length of the CE was less in the simulation with $\varepsilon_0=10\%$ because the SEE was extended 7.5 mm more than in the simulation with $\varepsilon_0=4\%$, giving an extra 5.6 J of stored elastic energy (remember that this energy originates from the CE).

Note that, initially, soleus MTC length increases, while soleus CE length does not. This means that other muscles are doing work on the SEE of the soleus, which is stored as elastic energy. When the soleus becomes activated, the CE starts to shorten. Initially, energy is put into the tendon by the CE (force increases); later, energy is released from the tendon (force decreases). In the simulation with $\varepsilon_0=10\%$, the shortening velocity of the soleus CE at any given CE length is lower than with $\varepsilon_0=4\%$ (Fig. 5C), and this allows the CE to do more work (i.e. the area under the CE length/force curve) despite its smaller shortening range. The lower shortening velocity of the CE is due to the larger contribution of the SEE to MTC shortening. Take-off occurs when the soleus force has fallen to zero, indicating that all elastic energy stored in the SEE is released, including the extra energy stored initially at $\varepsilon_0=10\%$.

In addition to the increase in work output of the soleus of 12.5 J, the work output of the vasti, rectus femoris and gluteus
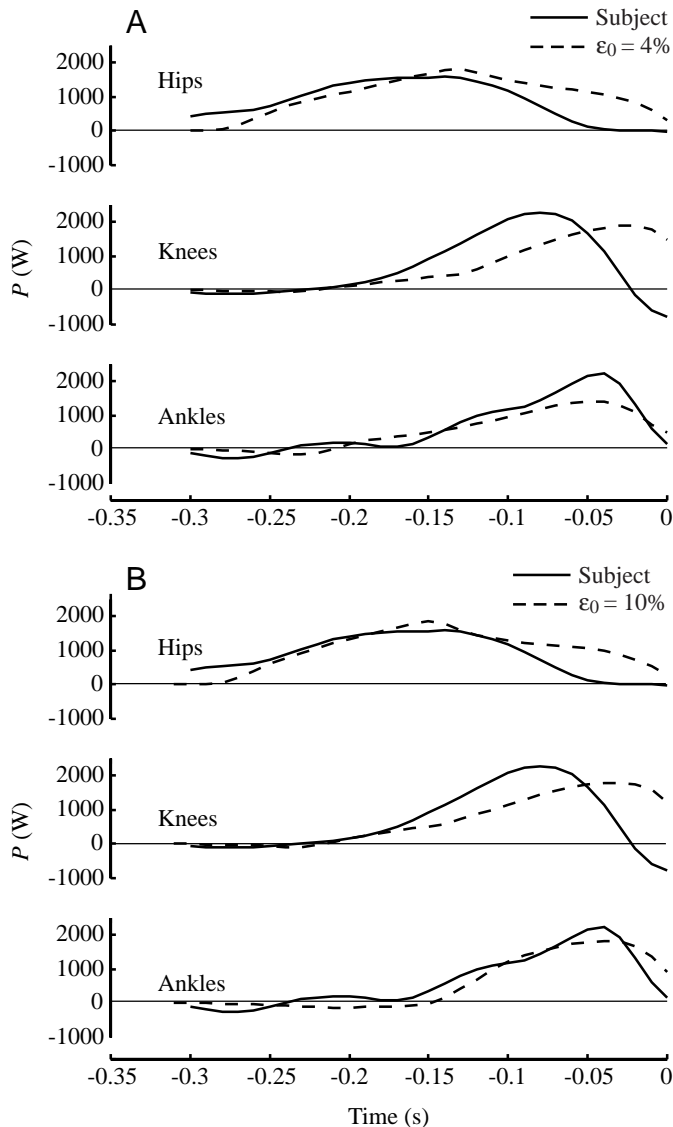
Fig. 4. Time histories of net joint power production (*P*) for the push-off in maximum-height squat jumping for a subject (solid lines) and for the optimal solution of the simulation model (broken lines) with the strain at isometric force ε_0 of the series elastic elements of the triceps surae set to 4 % (A) or 10 % (B). Take-off is at $t=0$ s.

Fig. 5. Force production (*F*) by the soleus plotted as function of the length of the muscle–tendon complex (MTC) (A), and force (B) and shortening velocity of contractile elements (V_{CE}) (C) plotted as a function of length of the contractile element (CE), for the optimal solution of the model with the strain at isometric force ε_0 of the series elastic elements of the triceps surae set to 4 % (solid lines) or 10 % (broken lines). Take-off is at $t=0$ s. The dotted parabola in B represents the maximal isometric force that can be produced at maximum active state and zero V_{CE}. The arrows indicate the progress of time.

maximus together also increased by 9.1 J when the ε_0 of the triceps surae SEE was increased from 4 to 10 %. In the case of the vasti and gluteus maximus, this was partly due to a lower CE shortening velocity and partly to a slightly greater CE shortening distance, which arose from differences in the state of the system at take-off (Table 4, see below).

Why does a change in SEE compliance of the triceps surae affect efficacy?

As described above, a higher vertical velocity at take-off occurs in the optimal jump with $\varepsilon_0=10$ % than in that with $\varepsilon_0=4$ % (Fig. 2). The vertical velocity of the CM is produced by rotations of the segments. Thus, at first glance, one would expect the angular velocity of the segments, and therewith the
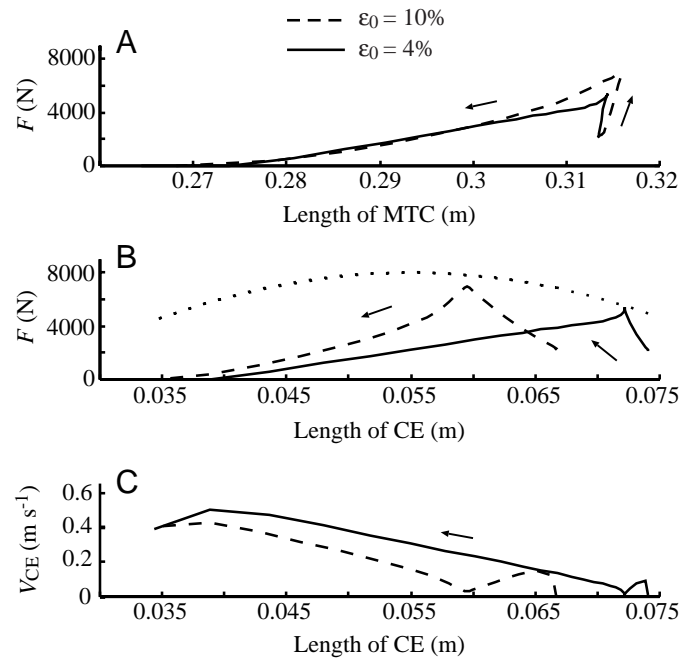
rotational energy (Table 2), to be higher at take-off when $\varepsilon_0=10$ %; in fact, the opposite was true, it was 8 J lower. The same was true for the horizontal kinetic energy of the segments relative to the CM, which was 4 J lower with $\varepsilon_0=10$ % (results not shown). This means that a larger fraction of the work produced at $\varepsilon_0=10$ % is converted into effective energy, i.e. energy contributing to jump height. How is this possible? The answer must lie in the contribution of rotations of the individual segments to the vertical velocity of the CM. In a given configuration of the system, the same linear velocity of the CM can by achieved by different combinations of angular velocities of the segments. To minimize rotational energy, the angular velocities of segments with a small moment of inertia, such as the feet, should be as large as possible, and those of segments with larger moments of inertia, such as the HAT, should be minimised. Thus, generally speaking, for a given amount of input energy, a greater amount of effective energy can be achieved if the contribution of the distal segments to the vertical velocity of the CM can be increased and that of the proximal segments decreased. A shift in these contributions could explain why increasing the ε_0 of the triceps surae SEE from 4 to 10 % results in a higher efficacy, as shown by the following analysis.

As argued previously (Bobbert and van Ingen Schenau,

1988), the contribution of segment i (where $i=1$ is the feet, $i=2$ is the shanks, $i=3$ is the thighs and $i=4$ is the HAT) may be written as:

$$\dot{z}_{CM,contr,i} = \frac{m_i}{m_{tot}} d_i \cdot \cos\varphi_i \cdot \dot{\varphi}_i + \sum_{j=i+1}^{4} \frac{m_j}{m_{tot}} l_i \cdot \cos\varphi_i \cdot \dot{\varphi}_i , \quad (2)$$

where $\dot{z}_{CM,contr,i}$ is the contribution of rotation of segment i to the vertical velocity of CM, m_i is the mass of segment i, m_j is the mass of segment j, m_{tot} is the total mass of the system, d_i is the distance between the centre of mass of the segment and the caudal end of this segment, l_i is the length of the segment, φ_i is the angle of the segment with the right-hand horizontal (see definition in Fig. 1) and $\dot{\varphi}_i$ is the angular velocity of the segment. Note that the rotation of each segment contributes in two ways to the vertical velocity of the CM: first because it affects the linear motion of the CM of the segment itself (first term on the right-hand side of equation 2) and second because it affects the linear motion of all the segments above its cranial end (second term on the right-hand side of equation 2).

Fig. 6 shows the time histories of the segmental contributions to the vertical velocity of the CM for the two simulated jumps at $\varepsilon_0=4\%$ and $\varepsilon_0=10\%$. The contributions sum up to give the CM vertical velocities presented in Table 2. Note that the feet start to contribute later in the condition $\varepsilon_0=10\%$. This is only partly due to the later stimulation onset of the plantar flexors. The major reason is that, because of the increased compliance, the plantar flexion moment builds up more slowly, so that it takes longer before the centre of pressure arrives at the ball of the foot, and hence it takes longer before foot rotation starts. After initially lagging behind, the $\dot{z}_{CM}$ contributions of the feet and lower legs rapidly increase to reach higher values at take-off for $\varepsilon_0=10\%$ than for $\varepsilon_0=4\%$. The reverse is true for the contributions of rotation of the thighs and HAT. Obviously, the contribution of segment i is proportional to $\cos\varphi_i \cdot \dot{\varphi}_i$.

Table 4 presents information on the state of the segments at take-off for the simulated jumps with $\varepsilon_0=4\%$ and $\varepsilon_0=10\%$. By virtue of the higher $\dot{z}_{CM}$ contributions of the feet and shanks at take-off, the vertical velocity of the CM at take-off can be
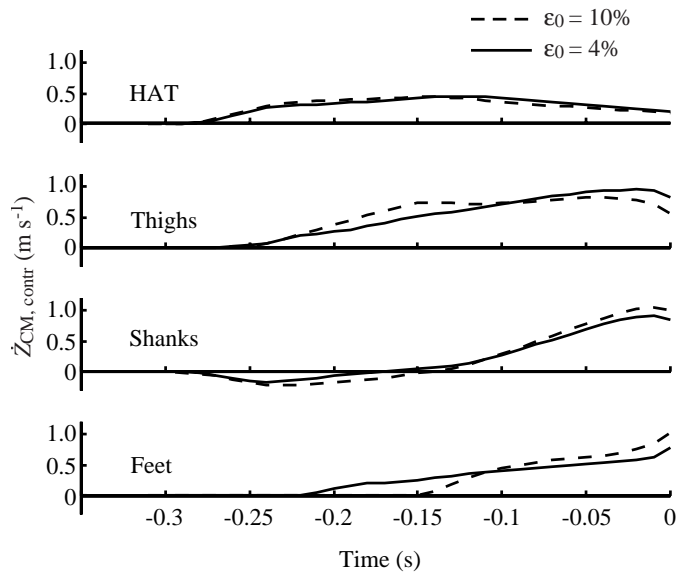

Fig. 6. Time histories of the contributions of segmental rotations to the vertical velocity of the centre of mass ($\dot{z}_{CM,contr}$) for the optimal solution of the model with the strain at isometric force ε_0 of the series elastic elements of the triceps surae set to 4% (solid lines) or 10% (broken lines). HAT is the head, arms and trunk. Take-off is at $t=0$ s.

higher for $\varepsilon_0=10\%$ despite a lower (less negative) angular velocity of the thighs and, more importantly, a smaller angular velocity of the HAT segment (Table 4). Because these latter segments have larger moments of inertia than the feet and shanks, less energy is present in the form of rotational energy at take-off (Table 2). This redistribution of $\dot{z}_{CM}$ contributions, which occurs when the ε_0 of the triceps surae SEE is increased from 4 to 10%, explains the surprising combination of a lower rotational energy with a higher vertical velocity of the CM at take-off, and thus the increased efficacy at $\varepsilon_0=10\%$.

Above, it is deduced that the vertical velocity of CM at take-off is higher at $\varepsilon_0=10\%$ because of higher angular velocities of the feet and shanks, which together produce a higher angular velocity of the ankle at take-off. It follows that, in the phase

Table 4. *Values for variables representing the state of the body segments at take-off in the optimal jumps of the model with the strain at maximum isometric force ε_0 of series elastic elements of the triceps surae set to 4%*

		Feet	Shanks	Thighs	HAT	$\dot{z}_{CM,to}$
$\varepsilon_0=4\%$	φ_{to} (rad)	**1.98**	**1.38**	**1.81**	**1.35**	
	$\dot{\varphi}_{to}$ (rad s^{-1})	**−11.8**	**10.4**	**−9.2**	**4.5**	
	$\dot{z}_{CM,contr}$ (m s^{-1})	**0.77**	**0.84**	**0.83**	**0.20**	**2.65**
$\varepsilon_0=10\%$	φ_{to} (rad)	+0.05	−0.02	−0.08	−0.02	
	$\dot{\varphi}_{to}$ (rad s^{-1})	−2.4	+0.6	+0.1	−0.6	
	$\dot{z}_{CM,contr}$ (m s^{-1})	+0.26	+0.16	−0.27	−0.01	+0.13

Values obtained with $\varepsilon_0=10\%$ are expressed relative to those obtained at $\varepsilon_0=4\%$ (in bold type).

Note that, because the definitions of segment angles are with respect to the right horizontal (see Fig. 1), negative angular velocities of the feet and thighs correspond to 'extension'.

HAT, head, arms and trunk; φ_{to}, angle of segment with right horizontal (see Fig. 1B) at take-off; $\dot{\varphi}_{to}$, angular velocity of segment at take-off; $\dot{z}_{CM,contr}$, contribution of rotation of segment to the vertical velocity of the centre of mass $\dot{z}_{CM,to}$.
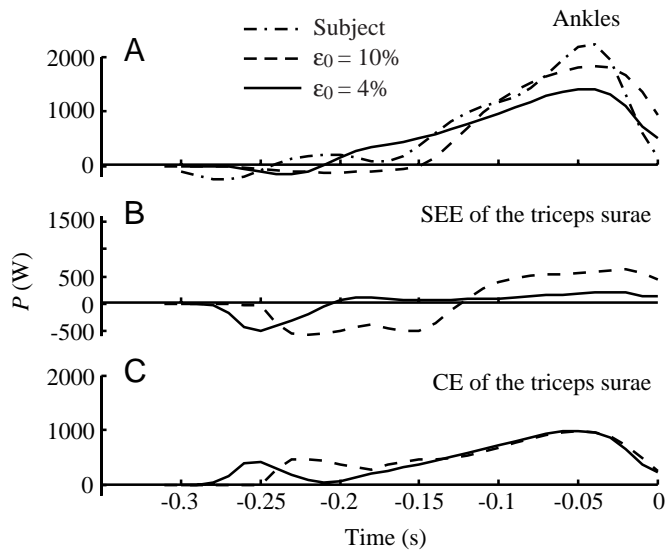
Fig. 7. Time histories of power output (*P*) at the ankles (A) and for the power contributions of the triceps surae series elastic element (SEE) (B) and contractile element (CE) (C) for the optimal solution of the simulation model with the strain at isometric force ε_0 of the series elastic elements of the triceps surae set to 4 % (solid lines) or 10 % (broken lines). In A, power output at the ankles measured in a subject during maximum-height squat jumping is also plotted. Values are for two legs together. Take-off is at *t*=0 s.

Table 5. *Contributions to the peak power output at the ankles during the simulated jumps*

		Soleus		Gastrocnemius		
	$P_{A,peak}$ (W)	P_{CE} (W)	P_{SEE} (W)	P_{CE} (W)	P_{SEE} (W)	P_{trans} (W)
ε_0=4 %	**1400**	**659**	**105**	**335**	**75**	**226**
ε_0=10 %	+400	−31	+284	−4	+119	+66

Absolute values are presented for the model with the strain at maximum isometric force ε_0 of the series elastic elements of the triceps surae set to 4 %.

Values obtained at ε_0=10 % are expressed relative to those obtained at ε_0=4 % (in bold type).

All values are for two legs together.

$P_{A,peak}$, peak power output about the ankles; P_{CE}, power output of contractile elements at the instant that $P_{A,peak}$ occurs; P_{SEE}, power output of series elastic elements at the instant that $P_{A,peak}$ occurs; P_{trans}, power transported (see Bobbert et al., 1986b) by the gastrocnemius from the knee to the ankle at the instant that $P_{A,peak}$ occurs.

preceding take-off, the system is able to achieve the same acceleration of the CM at a higher angular velocity of plantar flexion, indicating a higher power output at the ankle (Bobbert et al., 1986b). Time histories of power output at the ankle and the contributions of the CE and SEE of the triceps surae are shown in Fig. 7; Table 5 presents contributions to the peak power output at the ankle. It can be concluded from Fig. 7 that, during the last 120 ms before take-off, power output at the ankle is higher for ε_0=10 %, not because the power output of the CE is higher but primarily because energy release by the SEE is greater (see also Table 5). Energy released by the SEE during this phase was stored earlier in the push-off. Fig. 7 clearly shows how the SEE acts as a temporary energy buffer and also how the increased capacity of the buffer when ε_0=10 % helps to delay plantar flexion and increase the energy released during the last 120 ms of the push-off.

Why does an optimal SEE compliance exist?

Similar analyses to that presented above could be performed for the effects of increasing ε_0 from 1 to 4 %, or from 10 to 15 %, with more-or-less similar results (see Table 2). However, it is more interesting to analyse why performance is reduced when ε_0 is increased from 15 to 20 %. At these high values for SEE compliance, the CE is already below its optimum length at the start of the contraction and operates only on the ascending limb of its force/length relationship, below optimum length. Hence, it produces smaller peak forces and is unable to offset the disadvantage of a smaller shortening range. The optimal compliance of the SEE represents a trade-off between

storing as much energy as possible in the SEE while preserving the shortening range of the CE as much as possible.

Concluding remarks

The present study shows that the SEE compliance of the triceps surae has a considerable effect on the maximum height achieved in a squat jump. The effect was of the same magnitude as that presented previously (Pandy, 1990). It is mediated by changes in work output of both the triceps surae and other muscles and by changes in the efficacy of converting the work produced to energy that contributes to jump height. These changes are possible by virtue of the fact that increasing the capacity of the SEEs to store energy allows the system to achieve a higher power output at the ankles during the last part of the push-off. These findings support the hypotheses put forward in previous studies, in which kinematic measurements made during human jumping and muscle stimulation time histories were used as a starting point (Bobbert et al., 1986a; Bobbert et al., 1986b). Compliances of the magnitude measured by Hof (Hof, 1998), which correspond to an ε_0 of approximately 10 %, are necessary to explain the high power and work output about the ankle observed in human subjects performing vertical jumps (Fig. 4). Thus, long compliant tendons in the plantar flexors may have evolved as a solution to the problem of maximizing performance in tasks that involve explosive leg extension.

The advantage of SEE compliance in squat jumping arises from the temporary storage of energy in the SEE and its subsequent release at a high rate. In cyclic locomotor tasks involving stretch–shortening cycles, such as running and hopping, this buffering capacity allows for energy saving: during the stretch phase, superfluous kinetic and potential energy may partly be stored in the SEE and later re-utilized during the shortening phase (Cavagna, 1977). This mechanism

allows hopping animals to uncouple aerobic metabolic energy costs from locomotion speed (Biewener et al., 1998; Dawson and Taylor, 1973). Interestingly, the beneficial effect of SEE compliance of the triceps surae on the efficacy ratio in squat jumping, as described in the present study, also helps to save energy in cyclic locomotor tasks. It is then possible to achieve a given velocity of the CM at lower angular velocities of the proximal segments with large moments of inertia and, thereby, to achieve a given amount of effective energy with less wasted rotational energy.

References

Anderson, F. C. and Pandy, M. G. (1993). Storage and utilization of elastic strain energy during jumping. *J. Biomech.* **26**, 1413–1427.

Asmussen, E. and Bonde-Petersen, F. (1974). Apparent efficiency and storage of elastic energy in human muscles during exercise. *Acta Physiol. Scand.* **92**, 537–545.

Biewener, A. A., Konieczynski, D. D. and Baudinette, R. V. (1998). *In vivo* muscle force–length behavior during steady-speed hopping in tammar wallabies. *J. Exp. Biol.* **201**, 1681–1694.

Bobbert, M. F., Ettema, G. C. and Huijing, P. A. (1990). The force–length relationship of a muscle–tendon complex: experimental results and model calculations. *Eur. J. Appl. Physiol. Occup. Physiol.* **61**, 323–329.

Bobbert, M. F., Gerritsen, K. G., Litjens, M. C. and Van Soest, A. J. (1996). Why is countermovement jump height greater than squat jump height? *Med. Sci. Sports Exerc.* **28**, 1402–1412.

Bobbert, M. F., Huijing, P. A. and van Ingen Schenau, G. J. (1986a). A model of the human triceps surae muscle–tendon complex applied to jumping. *J. Biomech.* **19**, 887–898.

Bobbert, M. F., Huijing, P. A. and van Ingen Schenau, G. J. (1986b). An estimation of power output and work done by the human triceps surae muscle–tendon complex in jumping. *J. Biomech.* **19**, 899–906.

Bobbert, M. F. and van Ingen Schenau, G. J. (1988). Coordination in vertical jumping. *J. Biomech.* **21**, 249–262.

Cavagna, G. A. (1977). Storage and utilization of elastic energy in skeletal muscle. *Exerc. Sport Sci. Rev.* **5**, 89–129.

Dawson, T. J. and Taylor, C. R. (1973). Energetic cost of locomotion in kangaroos. *Nature* **246**, 313–314.

Elftman, H. (1939). Forces and energy changes in the leg during walking. *Am. J. Physiol.* **125**, 339–356.

Hatze, H. (1981). *A Myocybernetic Control Model of Skeletal Muscle*, pp. 31–42. Pretoria: University of South Africa.

Hill, A. V. (1938). The heat of shortening and the dynamic constants of muscle. *Proc. R. Soc. Lond. B* **126**, 136–195.

Hof, A. L. (1998). *In vivo* measurement of the series elasticity release curve of human triceps surae muscle. *J. Biomech.* **31**, 793–800.

Komi, P. V. and Bosco, C. (1978). Utilization of stored elastic energy in leg extensor muscles by men and women. *Med. Sci. Sports Exerc.* **10**, 261–265.

Kubo, K., Kawakami, Y. and Fukunaga, T. (1999). Influence of elastic properties of tendon structures on jump performance in humans. *J. Appl. Physiol.* **87**, 2090–2096.

Minetti, A. E., Ardig, O. L., Reinach, E. and Saibene, F. (1999). The relationship between mechanical work and energy expenditure of locomotion in horses. *J. Exp. Biol.* **202**, 2329–2338.

Out, L., Vrijkotte, T. G., van Soest, A. J. and Bobbert, M. F. (1996). Influence of the parameters of a human triceps surae muscle model on the isometric torque-angle relationship. *J. Biomech. Eng.* **118**, 17–25.

Pandy, M. G. (1990). An analytical framework for quantifying muscular action during human movement. In *Multiple Muscle Systems: Biomechanics and Movement Organization* (ed. J. M. Winters and S. L.-Y. Woo), pp. 653–662. New York: Springer.

Pandy, M. G., Zajac, F. E., Sim, E. and Levine, W. S. (1990). An optimal control model for maximum-height human jumping. *J. Biomech.* **23**, 1185–1198.

Svantesson, U., Ernstoff, B., Bergh, P. and Grimby, G. (1991). Use of a Kin-Com dynamometer to study the stretch–shortening cycle during plantar flexion. *Eur. J. Appl. Physiol.* **62**, 415–419.

van Ingen Schenau, G. J., Bobbert, M. F. and de Haan, A. (1997). Does elastic energy enhance work and efficiency in the stretch–shortening cycle? *J. Appl. Biomech.* **13**, 389–415.

van Ingen Schenau, G. J., Bobbert, M. F. and Rozendal, R. H. (1987). The unique action of bi-articular muscles in complex movements. *J. Anat.* **155**, 1–5.

van Soest, A. J. and Bobbert, M. F. (1993). The contribution of muscle properties in the control of explosive movements. *Biol. Cybernetics* **69**, 195–204.

van Soest, A. J., Schwab, A. L., Bobbert, M. F. and van Ingen Schenau, G. J. (1993). The influence of the biarticularity of the gastrocnemius muscle on vertical-jumping achievement. *J. Biomech.* **26**, 1–8.

Zajac, F. E. (1993). Muscle coordination of movement: a perspective. *J. Biomech.* **26**, 109–124.